Conversion of Aurivillius Phases $Bi_2ANaNb_3O_{12}$ (A = Sr or Ca) into the Protonated Forms of Layered Perovskite via Acid Treatment

Wataru Sugimoto,[†,§] Masashi Shirata,[†] Kazuyuki Kuroda,[†,‡] and Yoshiyuki Sugahara*[,†]

Department of Applied Chemistry, School of Science and Engineering, Waseda University, Ohkubo-3, Shinjuku-ku, Tokyo 169-8555, Japan, and Kagami Memorial Laboratory for Materials Science and Technology, Waseda University, Nishiwaseda-2, Shinjuku-ku, Tokyo 169-0051, Japan

Received November 9, 2001. Revised Manuscript Received April 10, 2002

Protonated forms of layered perovskites were derived from Aurivillius phases, $Bi_2ANaNb_3O_{12}$ (A = Sr or Ca), by the substitution of bismuth oxide sheets with protons via acid treatment. The conversion into the protonated forms was achieved easily using 6 M HCl at room temperature. Preservation of the structure of the perovskite-like slabs and contraction in the *c* axis were confirmed by X-ray and electron diffraction analysis as well as by transmission electron microscopy. The compositions of the resulting products were determined to be $H_{1.8}[A_{0.8}Bi_{0.2}NaNb_3O_{10}]$ (A = Sr or Ca) by inductively coupled plasma emission spectroscopy and thermogravimetry. The acid-treated product $H_{1.8}[Sr_{0.8}Bi_{0.2}NaNb_3O_{10}]$ was capable of accommodating *n*-alkylamines in the interlayer space, which is in good agreement with the proposed layered structure.

Introduction

Extensive research has recently been devoted to layered perovskites possessing ion-exchange capabilities. These compounds are expressed by the general formula $M_2[A_{n-1}B_nO_{3n+1}]$ (the so-called Ruddlesden−Popper phases[1]) or $M[A_{n-1}B_nO_{3n+1}]$ (the so-called Dion−Jacobson phases[2]), where M is an alkali metal ion, A is an alkaline-earth or rare-earth metal ion, and B is a transition metal ion. $[A_{n-1}B_nO_{3n+1}]$ denotes the perovskite-like slabs derived by termination of the three-dimensional ABO_3 perovskite structure along the (100) axis, which are interleaved with alkali metal ions, giving a characteristic layered structure. Typical three-layered structures are shown schematically in Scheme 1.

One of the unique characteristics of these oxides is that the interlayer alkali metal ions can be exchanged with other monovalent or divalent cations. For example, reactions of $M_2[A_{n-1}B_nO_{3n+1}]$ and $M[A_{n-1}B_nO_{3n+1}]$ with aqueous acids lead to their corresponding protonated forms $H_2[A_{n-1}B_nO_{3n+1}]$ and $H[A_{n-1}B_nO_{3n+1}]$ via a proton-exchange reaction ($M^+ \rightarrow H^+$).[2−4] These protonated forms of layered perovskites have drawn considerable interest across a wide range of chemistry fields because they exhibit numerous properties,[5] examples of which include ion-exchange capability,[6] Brønsted

Scheme 1. Schematic Structures of *n* = 3 Layered Perovskites[a]

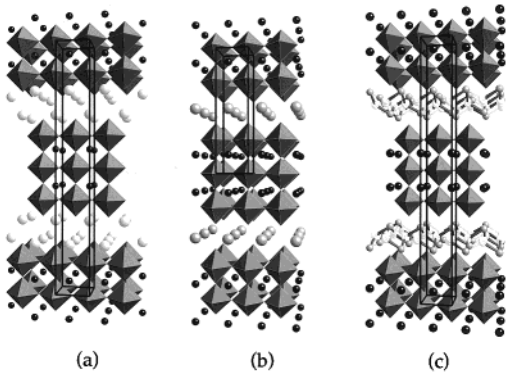

[a] (a) Ruddlesden−Popper phases $K_2[A_2B_3O_{10}]$, (b) Dion−Jacobson phases $Rb[A_2B_3O_{10}]$, and (c) Aurivillius phases $Bi_2O_2[A_2B_3O_{10}]$. The octahedrons represent the BO_6 units, and the black balls represent the 12-coordinated A-site cations in the perovskite-like slabs. The gray balls represent the interlayer K ions in (a) and the Rb ions in (b). The gray and white balls in (c) represent the bismuth and oxygen ions in the bismuth oxide sheets, respectively.

* To whom correspondence should be addressed. E-mail: ys6546@waseda.ac.jp.
† School of Science and Engineering.
‡ Kagami Memorial Laboratory for Materials Science and Technology.
§ Current address: Department of Fine Materials Engineering, Faculty of Textile Science and Technology, Shinshu University, Tokida 3-15-1, Ueda, Nagano 386-8567, Japan.

(1) (a) Ruddlesden, S. N.; Popper, P. *Acta Crystallogr.* **1957**, *10*, 538. (b) Ruddlesden, S. N.; Popper, P. *Acta Crystallogr.* **1958**, *11*, 54.
(2) (a) Dion, M.; Ganne, M.; Tournoux, M. *Mater. Res. Bull.* **1981**, *16*, 1429. (b) Jacobson, A. J.; Johnson, J. W.; Lewandowski, J. T. *Inorg. Chem.* **1985**, *24*, 3727. (c) Dion, M.; Ganne, M.; Tournoux, M. *Rev. Chim. Miner.* **1986**, *23*, 61.
(3) Gopalakrishnan, J.; Bhat, V. *Inorg. Chem.* **1987**, *26*, 4299.
(4) (a) Ollivier, P. J.; Mallouk, T. E. *Chem. Mater.* **1998**, *10*, 2585. (b) Bhuvanesh, N. S. P.; Crosnier-Lopez, M.-P.; Duroy, H.; Fourquet, J.-L. *J. Mater. Chem.* **2000**, *10*, 1685.
(5) Jacobson, A. J. *Chemical Physics of Intercalation II*; P. Brenier: New York, 1993; p 117.
(6) For example, see: (a) Jacobson, A. J.; Johnson, J. W.; Lewandowski, J. T. *Mater. Res. Bull.* **1987**, *22*, 45. (b) Matsuda, T.; Fujita, T.; Miyamae, N.; Takeuchi, M.; Kunou, I. *J. Mater. Chem.* **1994**, *4*, 955.

10.1021/cm0115620 CCC: $22.00
Published on Web 06/04/2002

acidity,[2a,2c,6a,7−10] proton conduction,[11] and photochemical properties.[12] Various functional materials have also been derived from these protonated forms of layered perovskites, including intercalation compounds,[2b,2c,6a,7−9] alkoxyl derivatives,[13,14] porous materials,[12b,15] metastable three-dimensional perovskites,[4,16] and layer-by-layer assembly of exfoliated layered perovskites.[17]

The Aurivillius phases ($Bi_2A_{n-1}B_nO_{3n+3}$ or alternatively expressed as $Bi_2O_2[A_{n-1}B_nO_{3n+1}]$)[18] are also members of the layered perovskites, and extensive research has been devoted to their synthesis as well as the characterization of their ferroelectric property.[19] As shown in Scheme 1, the Aurivillius, Ruddlesden−Popper, and Dion−Jacobson phases all possess analogous perovskite-like slabs, $[A_{n-1}B_nO_{3n+1}]$. The major difference between the Aurivillius phases and the ion-exchangeable layered perovskites (Ruddlesden−Popper and Dion−Jacobson phases) is that the perovskite-like slabs are interleaved with bismuth oxide sheets in the former case and with alkali metal ions in the latter. Despite this structural similarity, the conversion of Aurivillius phases into related layered perovskites or vice versa has not been considered until recently.

We recently reported on the conversion of an Aurivillius phase, $Bi_2SrNaNb_3O_{12}$, to a protonated form of a layered perovskite by acid treatment.[20,21] The reaction involves a selective leaching of the bismuth oxide sheets with simultaneous proton incorporation into the interlayer space formed between the perovskite-like slabs. The incorporation of protons allows the preservation of charge neutrality and the two-dimensional characteristic of the layered perovskite structure. The resulting product is therefore similar to the protonated forms of layered perovskites obtained by the conventional proton-exchange reaction ($M^+ \rightarrow H^+$) for the Ruddlesden−Popper and the Dion−Jacobson phases. Acid treatment of an $n = 2$ member Aurivillius phase, $Bi_2SrTa_2O_9$, was conducted earlier by Suzuki et al.[22] They reported that an anisotropic structural modification occurred, but attributed the modification to the decomposition of the perovskite-like slabs. We have shown that acid treatment of $Bi_2SrTa_2O_9$ leads to $H_{1.8}[Sr_{0.8}Bi_{0.2}TaO_7]$ via selective leaching of the bismuth oxide sheets.[23] Another interesting reaction concerning the Aurivillius phases was recently reported by Gopalakrishnan et al.[24] Ruddlesden−Popper phases were converted into Aurivillius phases through metathesis reactions:

$$K_2[A_{n-1}B_nO_{3n+1}] \xrightarrow[800-900\ ^\circ C]{BiOCl} Bi_2O_2[A_{n-1}B_nO_{3n+1}] + 2KCl \quad (1)$$

The two correlated conversion reactions based on the Aurivillius phases establish a new general relationship between the Aurivillius phases and the ion-exchangeable layered perovskites.

Here, we report the details of the conversion of two $n = 3$ members of the Aurivillius phases, $Bi_2SrNaNb_3O_{12}$ and $Bi_2CaNaNb_3O_{12}$, into their corresponding protonated forms of layered perovskites. The reaction of $Bi_2SrNaNb_3O_{12}$ was reported in brief earlier.[20,21] The structures and compositions of the protonated forms as well as the mechanism of the conversion reaction will be compared and discussed with conventional proton-exchange reactions.

Experimental Section

Synthesis of $Bi_2ANaNb_3O_{12}$ (A = Sr or Ca). Polycrystalline $Bi_2SrNaNb_3O_{12}$ (BSNN) was prepared following a procedure similar to that employed for $Bi_{2.5}Na_{1.5}Nb_3O_{12}$[25] and $Bi_2CaNaNb_3O_{12}$.[26] BSNN was prepared by a solid-state reaction of a 1:1 mixture of $Bi_2SrNb_2O_9$ and $NaNbO_3$ at 1100 °C for 3 h. The calcination procedure was repeated after grinding to ensure a complete reaction. $Bi_2SrNb_2O_9$ was prepared in accordance with the procedures in a previous report.[27] $NaNbO_3$ was prepared from Na_2CO_3 and Nb_2O_5 by firing at 1000 °C for 1 h in air. The purity of $Bi_2SrNb_2O_9$ and $NaNbO_3$ was confirmed by powder X-ray diffraction (XRD, Mac Science MXP^3 diffractometer with monochromated Cu Kα radiation) and inductively coupled plasma emission (ICP) spectrometry (Nippon Jarrell Ash, ICAP 575 MARK II). Polycrystalline Bi_2-

(7) (a) Gopalakrishnan, J.; Bhat, V.; Raveau, B. *Mater. Res. Bull.* **1987**, *22*, 413. (b) Uma, S.; Raju, A. R.; Gopalakrishnan, J. *J. Mater. Chem.* **1993**, *3*, 709. (c) Gopalakrishnan, J.; Uma, S.; Bhat, V. *Chem. Mater.* **1993**, *5*, 132. (d) Uma, S.; Gopalakrishnan, J. *J. Solid State Chem.* **1993**, *102*, 332. (e) Uma, S.; Gopalakrishnan, J. *Chem. Mater.* **1994**, *6*, 907.

(8) Mohan Ram, R. A.; Clearfield, A. *J. Solid State Chem.* **1991**, *94*, 45.

(9) Nakato, T.; Nakade, M.; Kuroda, K.; Kato, C. *Stud. Surf. Sci. Catal.* **1994**, *90*, 285.

(10) Matsuda, T.; Fujita, T.; Miyamae, N.; Takeuchi, M.; Kanda, K. *Bull. Chem. Soc. Jpn.* **1993**, *66*, 1548.

(11) (a) Subramanian, M. A.; Gopalakrishnan, J.; Sleight, A. W. *Mater. Res. Bull.* **1988**, *23*, 837. (b) Mangamma, G.; Bhat, V.; Gopalakrishnan, J.; Bhat, S. V. *Solid State Ionics* **1992**, *58*, 303. (c) Sato, M.; Jin, T.; Uematsu, K. *J. Solid State Chem.* **1993**, *102*, 557. (d) Sato, M.; Abo, J.; Jin, T.; Ohta, M. *J. Alloys Compd.* **1993**, *192*, 81. (e) Thangadurai, V.; Shukla, A. K.; Gopalakrishnan, J. *Solid State Ionics* **1994**, *73*, 9.

(12) (a) Yoshimura, J.; Ebina, Y.; Kondo, J.; Domen, K.; Tanaka, A. *J. Phys. Chem.* **1993**, *97*, 1970. (b) Ebina, Y.; Tanaka, A.; Kondo, J. N.; Domen, K. *Chem. Mater.* **1996**, *8*, 2534. (c) Takata, T.; Furumi, Y.; Shinohara, K.; Tanaka, A.; Hara, M.; Kondo, J. N.; Domen, K. *Chem. Mater.* **1997**, *9*, 1063. (d) Takata, T.; Shinohara, K.; Tanaka, A.; Hara, M.; Kondo, J. N.; Domen, K. *J. Photochem. Photobiol.* **1997**, *106*, 45. (e) Nakato, T.; Ito, K.; Kuroda, K.; Kato, C. *Microporous Mater.* **1993**, *1*, 283.

(13) Matsuda, T.; Miyamae, N.; Takeuchi, M. *Bull. Chem. Soc. Jpn.* **1993**, *66*, 1551.

(14) Takahashi, S.; Nakato, T., Hayashi, S.; Sugahara, Y.; Kuroda, K. *Inorg. Chem.* **1995**, *34*, 5065.

(15) Matsuda, T.; Udagawa, M.; Kunou, I. *J. Catal.* **1997**, *168*, 26.

(16) (a) Richard, M.; Brohan, L.; Tournoux, M. *J. Solid State Chem.* **1994**, *112*, 345. (b) Gondrand, M.; Joubert, J.-C. *Rev. Chim. Miner.* **1987**, *24*, 33. (c) Byeon, S.-H.; Yoon, J.-J.; Lee, S.-O. *J. Solid State Chem.* **1997**, *127*, 119. (d) Schaak, R. E.; Mallouk, T. E. *J. Am. Chem. Soc.* **2000**, *122*, 2798.

(17) (a) Schaak, R. E.; Mallouk, T. E. *Chem. Mater.* **2000**, *12*, 2513. (b) Schaak, R. E.; Mallouk, T. E. *Chem Mater.* **2000**, *12*, 3427.

(18) (a) Aurivillius, B. *Ark. Kemi* **1949**, *1*, 463. (b) Aurivillius, B. *Ark. Kemi* **1949**, *1*, 499. (c) Aurivillius, B. *Ark. Kemi* **1950**, *2*, 519.

(19) For example, see: (a) Subbarao, E. C. *J. Am. Ceram. Soc.* **1962**, *45*, 166. (b) Subbarao, E. C. *J. Phys. Chem. Solids* **1962**, *23*, 665. (c) Wolfe, R. W.; Newnham, R. E. *J. Electrochem. Soc.* **1969**, *116*, 832. (d) Subbarao, E. C. *Ferroelectrics* **1973**, *5*, 267. (e) Kikuchi, T.; Watanabe, A.; Uchida, K. *Mater. Res. Bull.* **1977**, *12*, 299.

(20) Sugimoto, W.; Shirata, M.; Sugahara, Y.; Kuroda, K. *J. Am. Chem. Soc.* **1999**, *121*, 11601.

(21) Shirata, M.; Tsunoda, Y.; Sugimoto, W.; Sugahara, Y. *Materials Research Society Symposium Proceedings*, "Solid-State Chemistry of Inorganic Materials"; Geselbracht, M. J., Greedan, J. E., Johnson, D. C., Subramanian, M. A., Eds.; Materials Research Society: Warrendale, PA, 2001; Vol. 658, GG4.21.1.

(22) Suzuki, M.; Nagasawa, N.; Machida, A.; Ami, T. *Jpn. J. Appl. Phys.* **1996**, *35*, L564.

(23) Tsunoda, Y.; Shirata, M.; Sugimoto, W.; Liu, Z.; Terasaki, O.; Sugahara, Y.; Kuroda, K. *Inorg. Chem.* **2001**, *40*, 5768.

(24) Gopalakrishnan, J.; Sivakumar, T.; Ramesha, K.; Thangadurai, V.; Subbanna, G. N. *J. Am. Chem. Soc.* **2000**, *122*, 6237.

(25) Kikuchi, T. *Mater. Res. Bull.* **1979**, *14*, 1561.

(26) Muramatsu, K.; Shimazu, M.; Tanaka, J.; Horiuchi, S. *J. Solid State Chem.* **1981**, *36*, 179.

(27) Ismunandar; Kennedy, B. J.; Gunawan; Marsongkohadi *J. Solid State Chem.* **1996**, *126*, 135.

$CaNaNb_3O_{12}$ (BCNN) was prepared similarly by the solid-state reaction of a 1:1 mixture of $Bi_2CaNb_2O_9$ and $NaNbO_3$.

The composition ratios of metals determined by ICP for BSNN and BCNN were consistent with the nominal ratios within the range of experimental error (see Table 1 in Results and Discussion). The XRD pattern of BSNN was successfully indexed based on a tetragonal cell. Structural refinement of BSNN was performed by the Rietveld analysis program RIETAN[28] using the space group *I*4/*mmm*. The final refined lattice parameters were $a = 0.39007(1)$ and $c = 3.2926(1)$ nm (Supporting Information available). The XRD pattern of BCNN was indexed on the basis of an orthorhombic cell. Structural refinement was performed using the space group *B*2*cb*. The final refined lattice parameters were $a = 0.54836(3)$, $b = 0.54585(4)$, and $c = 3.2731(1)$ nm (Supporting Information available).

Acid Treatment of $Bi_2ANaNb_3O_{12}$ (A = Sr or Ca). Typically, 1 g of BSNN or BCNN was treated with 200 cm^3 of 6 M HCl (M = mol dm^{-3}) at room temperature for 72 h to obtain acid-treated BSNN and BCNN. Acid treatment was conducted with various acid concentrations and reaction periods. The results for the acid-treated products presented throughout this paper are for the products treated with 6 M HCl for 72 h unless otherwise stated. The acid-treated products were collected either by filtration or by centrifugation. After being washed with deionized H_2O, the products were dried at room temperature or 120 °C.

Reaction of the Acid-Treated Product with Alkylamines. The product obtained by acid treatment of BSNN with 6 M HCl for 72 h was reacted with *n*-butylamine (C4A) or *n*-octylamine (C8A) in a 50% alkylamine/heptane mixture under reflux conditions. The products were washed with excess heptane and dried at room temperature.

Analyses. The XRD patterns of the acid-treated products were collected with a Mac Science MXP[3] diffractometer. The lattice parameters of the acid-treated products were refined by the nonlinear least-squares method. The cation ratios of the products were determined by ICP. The products were dissolved with a mixture of concentrated HNO_3 (5 cm^3), HF (5 cm^3), and concentrated HCl (10 cm^3) for the ICP measurements. After ≈30 mg of the products had been dissolved by heating in the mixed acid, the resultant solution was further diluted with 6 M HCl. Thermogravimetry (TG, Mac Science, TG-DTA 2000S) was performed under a constant flow of dry air with a heating rate of 10 °C min^{-1}. The structural characterization of the amine-treated products was conducted by XRD (Mac Science M03XHF[22] diffractometer) with Mn-filtered Fe Kα radiation. The morphology of the products was studied with a scanning electron microscope (SEM, HITACHI, S-2500). Transmission electron microscopy (TEM, Hitachi H-8100A) was operated at 200 kV.

Results and Discussion

Structural Evaluation by Diffraction Techniques. Figure 1 compares the XRD patterns of BSNN and BSNN treated with 6 M HCl for 72 h after drying at room temperature. After acid treatment, new diffraction peaks that could be indexed as a series of (00*l*) reflections were observed. In contrast to the appearance of new (00*l*) peaks, the positions of the (*hk*0) peaks were unchanged. The broadness of the (*hkl*) ($l \neq 0$) peaks compared to that of the (*hk*0) peaks suggests that stacking disorders are present in acid-treated BSNN. The (*hkl*) ($l \neq 0$) peaks of acid-treated BSNN sharpen slightly and shift to higher diffraction angles after being dried at 120 °C (Figure 1c).

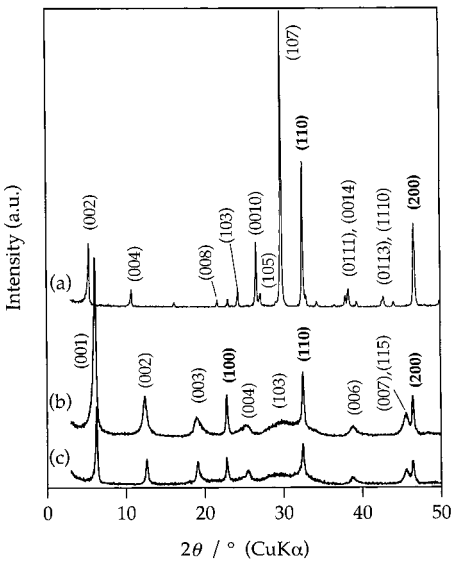

Figure 1. XRD patterns of (a) BSNN, (b) the room temperature dried product of BSNN treated with 6 M HCl for 72 h, and (c) the 120 °C dried product of BSNN treated with 6 M HCl for 72 h.

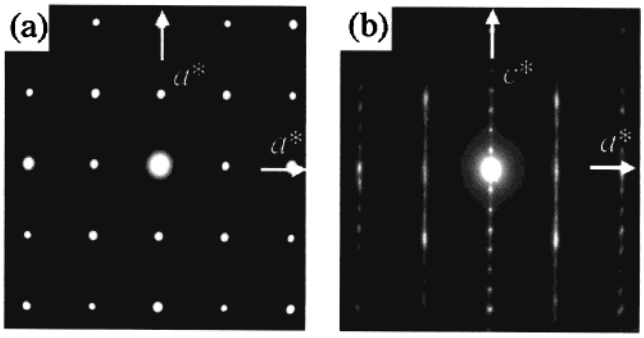

Figure 2. ED patterns along the [001] and [010] zones of (a) BSNN and (b) acid-treated BSNN obtained by 72-h treatment with 6 M HCl.

Electron diffraction (ED) analysis was conducted for BSNN and acid-treated BSNN to obtain further details concerning the structural changes. The ED patterns of BSNN and acid-treated BSNN were both indexed on the basis of a tetragonal cell. Typical ED patterns along the [001] and [010] zones are shown in Figure 2. The ED pattern along the [001] zone for acid-treated BSNN was essentially identical to that of BSNN and could be indexed on the basis of a tetragonal cell with $a \sim 0.39$ nm, which indicates that no structural change occurred along the *a* axes. On the other hand, the ED patterns along the [010] zone revealed a contraction in the *c* axis after acid treatment. In view of the facts that the (00*l*) planes are characteristic of a layered structure and that the (*hk*0) planes are characteristic of the perovskite-like slabs, it is concluded that acid treatment of BSNN leads to a structural transformation only along the *c* axis, while the perovskite-like structure is preserved along the *ab* plane, corresponding to the XRD results.

Electron Microscopy Studies. Typical SEM images of BSNN and acid-treated BSNN are shown in Figure 3. The size and platelike morphology are preserved after acid treatment, showing that the acid-treated product is not obtained by a dissolution−redeposition process. It is notable that the ED patterns along the [001] zone (Figure 2) were easily observable, while those along the

(28) (a) Izumi, F. *The Rietveld Method*; Young, R. A., Ed.; Oxford University Press: Oxford, 1993; pp 236−253. (b) Kim, Y. I.; Izumi, F. *J. Ceram. Soc. Jpn.* **1994**, *102*, 401.

Table 1. Cation Ratios of the Products

host compound	treatment time (h)	acid	molar ratio Bi	Sr	Ca	Na	Nb[a]
BSNN	0		2.00	1.00		1.02	3
BSNN	1	6 M HCl	1.55	0.94		0.99	3
BSNN	12	6 M HCl	0.27	0.75		1.00	3
BSNN	24	6 M HCl	0.29	0.79		0.99	3
BSNN	72	6 M HCl	0.21	0.80		1.00	3
BSNN	720	6 M HCl	0.19	0.74		0.95	3
BSNN	72	3 M HCl	0.22	0.76		0.99	3
BSNN	72	1 M HCl	1.83	0.96		1.04	3
BCNN	0		1.96		1.03	1.04	3
BCNN	72	6 M HCl	0.19		0.82	0.99	3

[a] Set to 3.

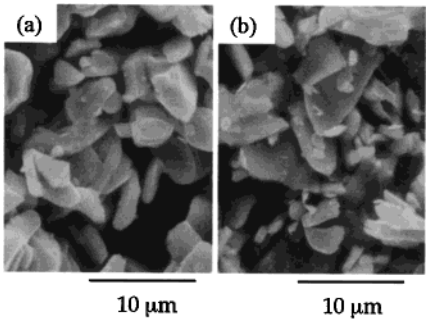

Figure 3. SEM images of (a) BSNN and (b) acid-treated BSNN obtained by 72-h treatment with 6 M HCl.

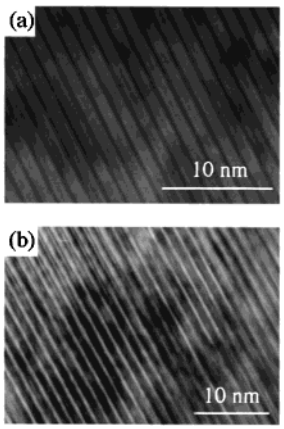

Figure 4. TEM images along the [010] zone of (a) BSNN and (b) acid-treated BSNN obtained by 72-h treatment with 6 M HCl.

[010] zone were much more difficult to observe. Such tendencies are due to the preferential cleavage plane along the *c* axis of the platelike morphology of the samples. Furthermore, characterization of numerous particles along the [001] zone revealed strong and well-resolved diffraction spots for the acid-treated product, indicating that no amorphous depositions were produced during acid treatment. The streaks along *c** suggest the presence of stacking disorders, which is consistent with the XRD results.

Typical [010] TEM images for BSNN and acid-treated BSNN are shown in Figure 4. Rows of dark and light contrast were observed at a periodicity of 1.6 nm for BSNN, which corresponds to *c*/2 of the unit cell. After acid treatment, the periodicity of the rows of dark and light contrasts decreased to 1.4 nm, which is consistent with the basal spacing observed by XRD and ED.

Compositional Evaluation. The cation ratios of BSNN treated with 6 M HCl for various treatment periods are summarized in Table 1. A dramatic decrease in the Bi/Nb ratio was observed upon acid treatment. In contrast, the Na/Nb ratio remained at unity regardless of the treatment conditions. A slight decrease in the Sr/Nb ratio upon acid treatment was also detected. These results indicate a selective leaching of Bi from BSNN. The composition of acid-treated BSNN was unchanged for treatments longer than 12 h, indicating that steady state was apparently obtained after 12 h of treatment. Even when extensive treatment lasting up to a month was conducted, a small amount of bismuth, coupled with a decrease in strontium content, was always detected. The progressive change in cation ratios as a function of treatment time was in good agreement with the structural transformation obtained by XRD (Supporting Information available).

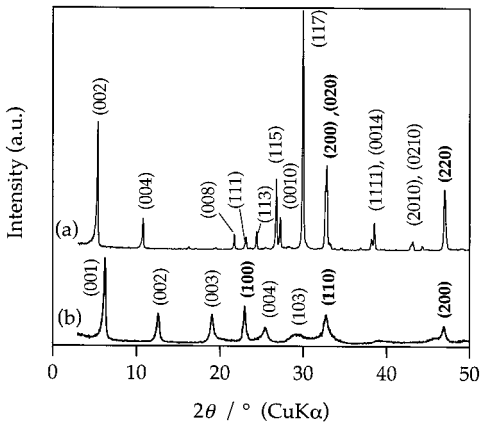

Figure 5. XRD patterns of (a) BCNN and (b) acid-treated BCNN obtained by 72-h treatment with 6 M HCl, followed by drying at 120 °C.

Compositional analysis of a supernatant solution was also conducted. The amount of Nb in the supernatant solution was <0.1 mass % of the initial mass of Nb used for the reaction (≈0.07 mg of Nb detected from an initial ≈353 mg of Nb in 1000 mg of BSNN). Because the results of the diffraction and microscopy analyses indicated that no amorphous materials were produced as a result of acid treatment, the cation ratios obtained by ICP can be taken as the composition of the perovskite-like slabs in acid-treated BSNN.

Acid Treatment of BCNN. Acid treatment of $Bi_2CaNaNb_3O_{12}$, the Ca analogue of BSNN, was also conducted. Figure 5 compares the XRD patterns of BCNN and BCNN treated with 6 M HCl for 72 h and dried at 120 °C. The structural transformation observed after acid treatment of BCNN was similar to that observed after acid treatment of BSNN; new diffraction peaks that could be indexed as a series of (00*l*) reflections were observed, while the positions of the (*hk*0) peaks were unchanged. The cation ratios of acid-treated BCNN are summarized in Table 1. The changes in the cation ratios after acid treatment indicate a selective leaching of Bi from BCNN. Partial loss of Ca and a small amount of undissolved Bi was also detected, similar to the observation for acid treatment of BSNN.

Reactions during Acid Treatment of BSNN and BCNN. Figure 6 shows the TG curves of $H_{1.8}[Bi_{0.2}Sr_{0.8}NaNb_3O_{10}]$ and $H_{1.8}[Bi_{0.2}Ca_{0.8}NaNb_3O_{10}]$, the products obtained by treatment of BSNN and BCNN with 6 M HCl for 72 h. The samples were dried at 120 °C to avoid

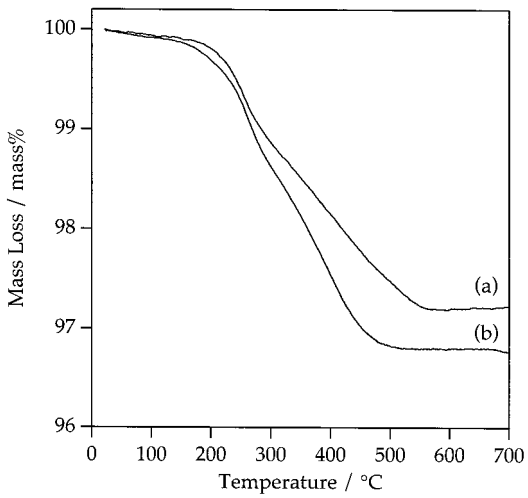

Figure 6. TG curves of the products obtained by acid treatment of (a) BSNN and (b) BCNN with 6 M HCl for 72 h, followed by drying at 120 °C.

the influence of adsorbed and/or interlayer water. The shape of the TG curves closely resembles those of protonated forms of layered perovskites obtained by conventional ion-exchange reactions with similar composition, such as $HCa_2Nb_3O_{10}$,[7c,8,11c] $H_2La_2Ti_3O_{10}$,[11e] and $H_2Sr_{1.5}Nb_3O_{10}$.[4b] The observed mass loss of 2.7 mass % between ≈160 and ≈550 °C can be attributed to dehydroxylation, which is in excellent agreement with the anticipated mass loss of 2.8 mass% according to the following equation:

$$H_{1.8}[Bi_{0.2}Sr_{0.8}NaNb_3O_{10}] \xrightarrow{\Delta} Bi_{0.2}Sr_{0.8}NaNb_3O_{9.1} + 0.9H_2O \quad (2)$$

Accordingly, the observed mass loss of 3.1 mass % between ≈130 and ≈550 °C corresponds to the anticipated mass loss of 3.0 mass % according to the following equation:

$$H_{1.8}[Bi_{0.2}Ca_{0.8}NaNb_3O_{10}] \xrightarrow{\Delta} Bi_{0.2}Ca_{0.8}NaNb_3O_{9.1} + 0.9H_2O \quad (3)$$

The slight amounts of residual bismuth and lost strontium (or calcium) in $H_{1.8}[Bi_{0.2}Sr_{0.8}NaNb_3O_{10}]$ (or $H_{1.8}[Bi_{0.2}Ca_{0.8}NaNb_3O_{10}]$) can be understood on the basis of the partial occupancy of Bi in the A site of the perovskite-like slabs of the host compounds, BSNN and BCNN. Partial disordering of Bi in the bismuth oxide sheets and the A-site cation in the perovskite-like slabs (Bi ↔ A) has been reported for $n = 2$ members of Aurivillius phases $Bi_2AB_2O_9$ (A = Ca, Sr, Ba, Pb, B = Nb, Ta).[29] It therefore seems natural to assume that similar disordering also exists in BSNN and BCNN. It is worth noting that this process can provide quantitative information for the cation disorders in the Aurivillius phases. Because the type of A-site cation in the Aurivillius phases affects their ferroelectric properties,[30] this process appears to be a valuable approach to the structural characterization of the Aurivillius phases.

Assuming that the residual bismuth is due to a disorder of cations, the overall reaction could be expressed as

$$(Bi_{1.8}A_{0.2}O_2)^{1.8+}[Bi_{0.2}A_{0.8}NaNb_3O_{10}]^{1.8-} \xrightarrow{\text{aq. HCl}} {}^{+}_{1.8}H[Bi_{0.2}A_{0.8}NaNb_3O_{10}]^{1.8-}\cdot nH_2O \quad (A = Sr \text{ or } Ca) \quad (4)$$

where n denotes interlayer and/or surface adsorbed water (typically $n = 0.4$ for an air-dried sample).[31]

Accordingly, the overall reaction can be regarded as the replacement of the positively charged bismuth oxide sheets (containing Sr or Ca) with protons to compensate for the negatively charged perovskite-like slabs ($\{(Bi_{1.8}A_{0.2}O_2)^{1.8+}\}_x \rightarrow 1.8xH^+$, where A = Sr or Ca). The reaction is schematically shown in Scheme 2. This should be compared with the proton-exchange reaction ($M^+ \rightarrow H^+$) in ion-exchangeable layered perovskites.

Mechanism of Selective Leaching. Protonated layered perovskites that possess perovskite-like slab compositions similar to $H_{1.8}[Bi_{0.2}Sr_{0.8}NaNb_3O_{10}]$ and $H_{1.8}[Bi_{0.2}Ca_{0.8}NaNb_3O_{10}]$ have been reported, for example, $H[BiNb_2O_7]$, $H[A_2Nb_3O_{10}]$ (A = Sr or Ca), $H_2[A_{1.5}Nb_3O_{10}]$ (A = Sr or Ca), and $H[Ca_2NaNb_4O_{13}]$.[2b,4b,9,12e] These were obtained by ion-exchange reactions using concentrated acids at 60 °C for a few days. These conditions are similar to or more severe than the conditions applied in this study. These previous results, combined with the fact that the process in this study involves no dissolution of Nb (as shown by the ICP results of the supernatant solution), show the relatively high stability of the Nb-based perovskite-like slabs in Aurivillius phases toward acid treatment under the present experimental conditions. The bismuth oxide sheets in the Aurivillius phases, on the other hand, are isostructural to those in the Sillén phase BiOCl, which is also a lamellar oxide.[32] BiOCl is known to be soluble in acidic solutions.[33] The selective leaching of the bismuth oxide sheets can be therefore understood on the basis of differences in the stabilities of the perovskite-like slabs and the bismuth oxide sheets in acidic solutions.

The use of high acid concentrations such as 6 M HCl is not necessarily a prerequisite for complete conversion. Identical ICP results (Table 1) and XRD results (not shown) can be achieved under milder conditions, such as by using 3 M HCl for 72 h. Even with 1 M HCl, a slight decrease in the Bi/Nb ratio was detected after treatment for 72 h, suggesting that the conversion

(29) (a) Srikanth, V.; Idink, H.; White, W. B.; Subbarao, E. C.; Rajagopal, H.; Sequeira, A. *Acta Crystallogr.* **1996**, *B52*, 432. (b) Blake, S. M.; Falconer, M. J.; McCreedy, M.; Lightfoot, P. *J. Mater. Chem.* **1997**, *7*, 1609. (c) Ismunandar; Hunter, B. A.; Kennedy, B. J. *Solid State Ionics* **1998**, *112*, 281. (d) Ismunandar; Kennedy, B. J. *J. Mater. Chem.* **1999**, *9*, 541. (e) Macquart R.; Kennedy, B. J.; Shimakawa, Y. *J. Solid State Chem.* **2001**, *160*, 174.

(30) Park B. H.; Kang, B. S.; Bu, S. D.; Noh, T. W.; Lee, J.; Jo, W. *Nature* **1999**, *401*, 682.

(31) For a typical reaction of BSNN conversion to acid-treated BSNN (72-h treatment with 6 M HCl at room temperature), 55.9 mass % of solid was recovered after the treatment (0.7580 g of BSNN → 0.4240 g of acid-treated BSNN). Because the theoretical change due to the reaction according to eq 2 is 57.8 mass % when $n = 0.4$, the observed mass change amounts to a ≈97% yield for the conversion.

(32) Sillén, L. G. *Z. Anorg. Allg. Chem.* **1941**, *246*, 331.

(33) (a) *A Dictionary of Chemical Solubilities: Inorganic, 2nd ed.*; Comey, A. M., Hahn, D. A., Eds.; MacMillan: New York, 1921. (b) *CRC Handbook of Chemistry and Physics*, 64th ed.; Weast, R. C., Astle, M. J., Beyer, W. H., Eds.; CRC Press: Boca Raton, FL, 1983.

Scheme 2. Schematic Representation of the Conversion of the Aurivillius Phases $Bi_2ANaNb_3O_{12}$ (A = Sr or Ca) to the Corresponding Protonated Forms of Layered Perovskite $H_{1.8}Bi_{0.2}A_{0.8}NaNb_3O_{10}$ (A = Sr or Ca) by the Bismuth Oxide Sheet to Proton Substitution Reaction

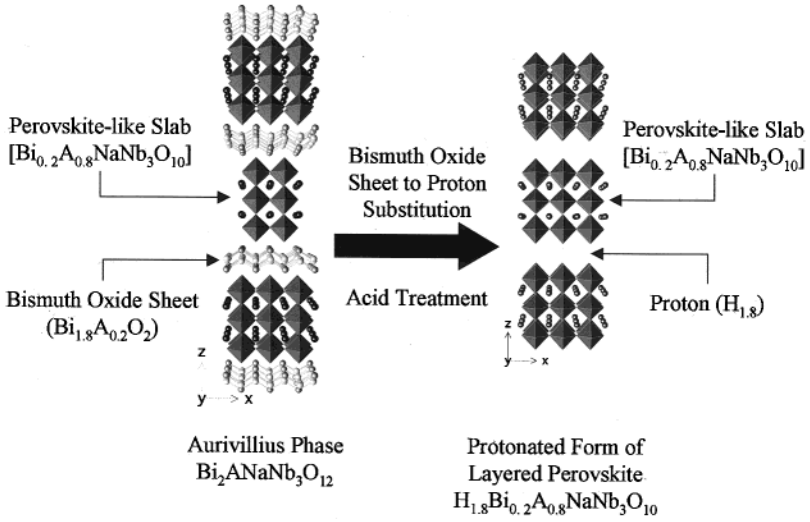

reaction may progress at lower acid concentrations with extended treatment.

Structural Consideration of the Acid-Treated Products. Because the characteristic two-dimensional structures of BSNN and BCNN were preserved in the acid-treated products, the structures of $H_{1.8}[Bi_{0.2}Sr_{0.8}NaNb_3O_{10}]$ and $H_{1.8}[Bi_{0.2}Ca_{0.8}NaNb_3O_{10}]$ should be closely related to those of the host compounds. Initially, indexing of the XRD pattern of $H_{1.8}[Bi_{0.2}Sr_{0.8}NaNb_3O_{10}]$ (dried at 120 °C) was attempted using a tetragonal cell with body-centered symmetry (*I*4/*mmm*) and $a \sim 0.39$, $c \sim 2.86$ nm. Although most of the peaks could be indexed, the sharp diffraction peak at $2\theta \sim 22.7°$ ($d \sim 0.39$ nm) could not be indexed reliably as the (103) peak ($2\theta_{(obs)} \sim 22.7°$; $2\theta_{(cal)} \sim 24.7°$). Moreover, we could not find any evidence for *c*-axis doubling in either the XRD or the ED patterns. The most reliable indexing of the XRD pattern for acid-treated BSNN was based on a primitive tetragonal symmetry with no *c*-axis doubling. In this case, the sharp diffraction peak at $2\theta \sim 22.7°$ could be reliably indexed as the (100) diffraction peak ($2\theta_{(obs)} \sim 22.7°$; $2\theta_{(cal)} \sim 22.7°$). The refined lattice parameters for $H_{1.8}[Bi_{0.2}Sr_{0.8}NaNb_3O_{10}]$ (dried at 120 °C) were $a = 0.391 \pm 0.002$ and $c = 1.39 \pm 0.02$ nm.[34] Likewise, the XRD pattern for $H_{1.8}[Bi_{0.2}Ca_{0.8}NaNb_3O_{10}]$ (dried at 120 °C) was indexed based on a primitive tetragonal symmetry with no *c*-axis doubling; the refined lattice parameters were $a = 0.390 \pm 0.003$ and $c = 1.41 \pm 0.01$ nm.

$H_2La_2Ti_3O_{10}$ obtained by ion exchange of the Ruddlesden−Popper phase $K_2La_2Ti_3O_{10}$ was reported to possess a structure with a relative displacement of the perovskite-like slabs by $(a + b)/2$, leading to a doubled *c* axis.[4] Although the host compounds, BSNN and BCNN, possess structures with doubled *c* axes, no doubling of the *c* axis was observed in the acid-treated products. Both the XRD [broadness of the (*hkl*) peaks] and ED (streaks along *c**) results for acid-treated BSNN indicate

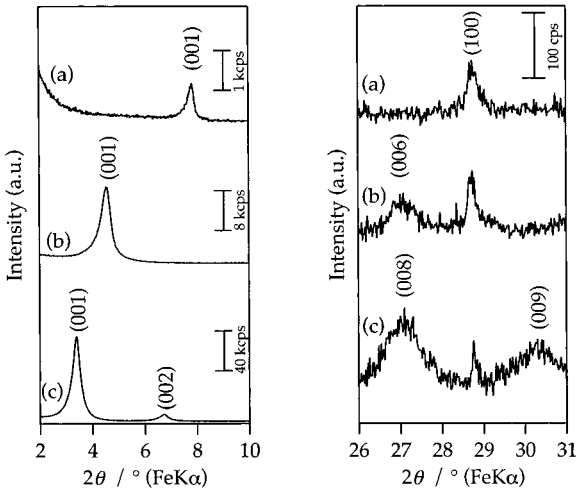

Figure 7. XRD patterns of (a) $H_{1.8}[Bi_{0.2}Sr_{0.8}NaNb_3O_{10}]$, (b) C4A−$H_{1.8}[Bi_{0.2}Sr_{0.8}NaNb_3O_{10}]$, and (c) C8A−$H_{1.8}[Bi_{0.2}Sr_{0.8}NaNb_3O_{10}]$.

the presence of stacking disorders, which should complicate the accurate determination of the cell symmetry and stacking sequence of the perovskite-like slabs by the powder XRD patterns. In fact, HREM observations of $H_{1.8}[Sr_{0.8}Bi_{0.2}Ta_2O_7]$ derived by a bismuth oxide sheet to proton substitution reaction of an $n = 2$ member of the Aurivillius phase, $Bi_2SrTa_2O_9$, indicated the existence of two types of perovskite-like slab stacking: a stacking sequence with no displacement of the perovskite-like slabs (*P*-type) and a stacking sequence with relative displacement by $(a + b)/2$ (*I*-type).[23] In contrast, the XRD pattern of $H_{1.8}[Sr_{0.8}Bi_{0.2}Ta_2O_7]$ was indexed based on a structure without displacement of the perovskite-like slabs. These observations indicate the presence of more than one local interlayer environment that cannot be detected by XRD in acid-treated BSNN. The indexing for $H_{1.8}[Bi_{0.2}Sr_{0.8}NaNb_3O_{10}]$ and $H_{1.8}[Bi_{0.2}Ca_{0.8}NaNb_3O_{10}]$ based on a primitive cell without *c*-axis doubling consequently represents only the "average structure", disregarding the local stacking sequence of the perovskite-like slabs.

(34) It is noted that the *c* lattice parameter was sensitive to the measurement environment. The *c* lattice parameter of the 120 °C dried product was slightly smaller than that of the room temperature dried product (see Table 2). Also, when the product was measured in a half-wet slurry state, the (001) peak was observed at $2\theta = 5.84°$ ($d = 1.51$ nm) with a shoulder peak at $2\theta = 5.32°$ ($d = 1.66$ nm).

Table 2. Lattice Parameters of the Aurivillius Phases, the Corresponding Protonated Forms, and Intercalation Compounds[a]

composition	*a* (nm)	*c* (nm)	ref
$Bi_2SrNaNb_3O_{12}$	0.39007(1)	1.6463(1)[e]	this work
$Bi_2CaNaNb_3O_{12}$	0.38686(3)[d]	1.6365(1)[e]	this work
$H_{1.8}[Bi_{0.2}Sr_{0.8}NaNb_3O_{10}]\cdot nH_2O$[b]	0.390(1)	1.43(2)	20
$H_{1.8}[Bi_{0.2}Sr_{0.8}NaNb_3O_{10}]$[c]	0.391(2)	1.39(2)	this work
$H_{1.8}[Bi_{0.2}Ca_{0.8}NaNb_3O_{10}]$[c]	0.390(3)	1.41(1)	this work
C4A$-H_{1.8}[Bi_{0.2}Sr_{0.8}NaNb_3O_{10}]$	0.390	2.43	this work
C8A$-H_{1.8}[Bi_{0.2}Sr_{0.8}NaNb_3O_{10}]$	0.390	3.26	this work
C4A$-H[Ca_2Nb_3O_{10}]$	0.3855	2.4952	6a
C8A$-H[Ca_2Nb_3O_{10}]$	0.3854	3.1514	6a

[a] The lattice parameters of the host Aurivillius phases were refined by Rietveld analysis. The lattice parameters of the protonated forms were refined by the nonlinear least-squares method. The *a* and *c* lattice parameters of the intercalation compounds were calculated from the (100) and (001) diffraction peaks, respectively. [b] Dried at room temperature. [c] Dried at 120 °C. [d] For the sake of comparison, the lattice parameter was reduced to $a_p = (a + b)/\sqrt{2}$ because of the difference in structure. [e] For the sake of comparison, the lattice parameter was reduced to *c*/2 because of the difference in structure.

Intercalation Chemistry of $H_{1.8}[Bi_{0.2}Sr_{0.8}NaNb_3O_{10}]$. Because protonated forms of layered niobates are known to accommodate alkylamines,[5,9a,35] reaction of *n*-alkylamines with $H_{1.8}[Bi_{0.2}Sr_{0.8}NaNb_3O_{10}]$ was conducted. After the reaction of $H_{1.8}[Bi_{0.2}Sr_{0.8}NaNb_3O_{10}]$ with *n*-alkylamines, all of the (00*l*) diffraction peaks were shifted to higher diffraction angles, while the (*hk*0) diffraction peaks were observed at the same diffraction angles, indicating intercalation of *n*-alkylamines into the interlayer space of $H_{1.8}[Bi_{0.2}Sr_{0.8}NaNb_3O_{10}]$ (Figure 7). The lattice parameters of C4A- and C8A-intercalated $H_{1.8}[Bi_{0.2}Sr_{0.8}NaNb_3O_{10}]$ were in good agreement with C4A- and C8A-intercalated $HCa_2Nb_3O_{10}$,[2b,6a] as summarized in Table 2. Chemical analysis revealed that 0.9 mol of C4A (C, 8.0 mass %; H, 1.9 mass %; N, 1.7 mass %) and 1.0 mol of C8A (C, 14.7 mass %; H, 3.1 mass %; N, 2.0 mass %) per $[Bi_{0.2}Sr_{0.80}NaNb_3O_{10}]$ were intercalated. To the best of our knowledge, this is the first evidence of intercalation of alkylamines into layered perovskites where the perovskite-like slabs possess a charge higher than 1.[36]

(35) Mallouk, T. E.; Kim, H.-N.; Ollivier, P. J.; Keller, S. W. *Comprehensive Supramolecular Chemistry Vol. 7*; Alberti, G., Bein, T., Eds.: Elsevier Science: Oxford, UK, 1996; pp 189−217.

(36) After our communication (ref 20), the intercalation of tetra(*n*-butyl)ammonium and exfoliation of a number of Ruddlesden−Popper phases (perovskite-like slabs possess a charge of 2) was reported by R. E. Schaak and T. E. Mallouk (ref 17a).

Conclusions

We have developed a novel method for obtaining protonated forms of layered perovskites derived from the Aurivillius phases. The structural and compositional analyses revealed that $H_{1.8}[Bi_{0.2}Sr_{0.8}NaNb_3O_{10}]$ and $H_{1.8}[Bi_{0.2}Ca_{0.8}NaNb_3O_{10}]$ were derived through acid treatment of $Bi_2SrNaNb_3O_{12}$ and $Bi_2CaNaNb_3O_{12}$, respectively. The bismuth oxide sheet to proton substitution reaction of the Aurivillius phases involves selective leaching of the bismuth oxide sheets accompanied by the introduction of interlayer protons ($\{(Bi_{1.8}A_{0.2}O_2)^{1.8+}\}_x \rightarrow 1.8xH^+$), a reaction resembling the conventional proton-exchange reaction ($M^+ \rightarrow H^+$). The small amount of residual Bi in the acid-treated product was suggested to result from the partial occupancy of Bi in the A site of the perovskite-like slabs in the Aurivillius phases, that is, $Bi_{1.8}A_{0.2}O_2[Bi_{0.2}A_{0.8}NaNb_3O_{10}]$ (A = Sr or Ca). The increase in basal spacing upon reaction of $H_{1.8}[Bi_{0.2}Sr_{0.8}NaNb_3O_{10}]$ with *n*-alkylamines provides evidence for the preservation of the characteristic layered structure.

We propose that the Aurivillius phases can be considered as a new homologous series of oxides for preparing protonated forms of layered-perovskite-related oxides. Numerous Aurivillius phases have been reported with combinations of various elements and *n* values (A = Na, Ca, Bi, etc.; B = Nb, Ti, etc.; $1 \leq n \leq 8$).[18,19] The findings of Pb-substituted Aurivillius phases have given rise to an even larger number of new Aurivillius phases with varying perovskite-like slab charge density.[37] The novel method of converting Aurivillius phases into the protonated forms of the layered perovskites opens up the possibility of obtaining an extensive range of new compounds.

Acknowledgment. The authors thank Mr. Minekazu Fujiwara at the Materials Characterization Central Laboratory, Waseda University, for the TEM observations. Experimental assistance by Mr. Yu Tsunoda and Ms. Fumi Nakasone is also acknowledged. This work was financially supported in part by the Grant-in-Aid for Scientific Research (No. 10555221) from the Ministry of Education, Science, Sports and Culture, Japan.

Supporting Information Available: The output from the Rietveld analysis, the crystallographic data obtained for $Bi_2SrNaNb_3O_{12}$ and $Bi_2CaNaNb_3O_{12}$, and the stacked plot for the variation in the XRD pattern as a function of reaction time (PDF). This material is available free of charge via the Internet at http://pubs.acs.org.

CM0115620

(37) Millán, P.; Castro, A.; Torrance, J. B. *Mater. Res. Bull.* **1993**, *28*, 117.